

## Observations of Repeating Earthquakes at a Single Seismic Station Near Lake Sapanca

Diğdem ACAREL<sup>1\*</sup>

<sup>1</sup>Gebze Technical University, Institute of Earth and Marine Sciences, Kocaeli

\*Corresponding Author e-mail: digdemacarel@gmail.com ORCID ID: <http://orcid.org/0000-0002-3179-6342>

Geliş Tarihi: 23 Nisan 2023 ; Kabul Tarihi: 12 Kasım 2023

### Abstract

The North Anatolian Fault Zone (NAFZ), which forms the plate boundary between Anatolian Plate and Eurasian Plate, is one of the most active transform fault zones in the world. Following two consecutive magnitude  $M>7$  earthquakes in 1999, an intensified monitoring of western portion of NAF is commenced. Dense networks of onshore/offshore seismic, acoustic, geodetic sensors and surface creep and strain sensors were installed. A single seismic sensor among these, which is located at the midpoint of 1999 ruptures, near Lake Sapanca, exhibits some unusual seismic activity. On a fault segment where creep is known to be present, a series of minor seismic events was observed with identical locations and a recurrence time of three years. These events are quite short in duration and highly similar in their waveforms. Using a single station approach, their angle of incidence and back azimuth were found to coincide with the location of two  $M2.3$  and  $M2.1$  events. At this stage, it is not clear whether these events reflect fault creep at seismogenic depth. Nevertheless, these initial observations emphasize the necessity of monitoring this segment more densely, where recurrent minor earthquakes are likely to be observed.

### Keywords

Lake Sapanca; North Anatolian Fault; Creep; Repeating Earthquakes; Single Seismic Station

## Sapanca Gölü Yakınında Tek Bir Sismik İstasyonda Tekrarlayan Deprem Gözlemleri

### Öz

Kuzey Anadolu Fay Zonu (KAFZ), Anadolu ve Avrasya plakaları arasındaki levha sınırını oluşturur ve dünya üzerindeki en aktif transform faylarından biridir. 1999'da meydana gelen iki  $M>7$  depremin ardından, KAF'ın batı kısmı yoğun bir şekilde izlenmeye başlanmıştır. Karada/denizde yoğun ağlarla sismik, akustik, jeodezik, yüzey kripi ve gerinimi ölçen sensörler kurulmuştur. Bu sensörler arasında, 1999 kırılmalarının merkezinde, Sapanca Gölü yakınlarında bulunan tek bir sismik sensör, bazı olağandışı sismik aktiviteler kaydetmiştir. Krip gözlemlenen bir fay segmentinde, aynı konumlarda, üç yıllık tekrarlama süresi ile küçük sismik olaylar gözlemlenmiştir. Bu olaylar oldukça kısa sürelidir ve dalga formları açısından oldukça benzerdir. Tek istasyon yaklaşımı kullanılarak, bu olayların çıkış açısı ve geri azimut açısının  $M2.3$  ve  $M2.1$  büyüklüğündeki depremlerin konumuna denk geldiği bulunmuştur. Bu aşamada, bu olayların sismojenik derinlikte kripi yansıtıp yansıtmadığı belirsizdir. Bununla birlikte, bu ilk gözlemler, tekrarlayan depremler gözlenen bu segmentin daha yoğun bir şekilde izlenmesinin gerekliliğini vurgulamaktadır.

### Anahtar kelimeler

Sapanca Gölü; Kuzey Anadolu Fayı; Krip; Tekrarlayan Depremler; Tek Bir Sismik İstasyon

© Afyon Kocatepe Üniversitesi

### 1. Introduction

The sudden release of accumulated tectonic stress along locked segments of major plate boundaries, resulting in large earthquakes and subsequent seismic hazard and risk, is the main interest of seismic studies. Recently, identifying creeping zones based on the observation of repeating earthquakes and episodic tremor and slip, attract considerable interest in order to derive more

reliable seismic hazard assessments as key input for risk mitigation and reduction strategies.

The North Anatolian Fault Zone (NAFZ), which accommodates the westward motion of Anatolian Plate with respect to stable Eurasia, is one of the most active bounding strike-slip faults in the world. Following the 1912 Ganos earthquake in the western Marmara region, this 1600 km long right

lateral strike slip fault has first ruptured in 1939 near Erzincan marking the beginning of a series of  $M > 7$  events migrating towards the Sea of Marmara in the west. In 1999, two large earthquakes occurred in Izmit-Gölcük ( $M7.4$ ) and Düzce ( $M7.1$ ), three months apart. The Izmit rupture is 140 km long and subdivided in four segments. The Düzce earthquake rupture is 40 km long, extending the rupture towards east (Barka *et al.* 2002). Subsequent to these two devastating earthquakes, the number of onshore and offshore sensors was increased around Sea of Marmara to better estimate the risk associated with the expected future major earthquake. As a result, many striking observations are made. On the western portion of the NAF propagating in Sea of Marmara, the Main Marmara Fault, repeating earthquakes were observed between the years 2008 and 2015 (Schmittbuhl *et al.* 2016). Later, spanning the years between 2006 and 2010, repeating earthquakes located in Central Basin were observed (Bohnhoff *et al.* 2017) (Figure 1a, yellow star). At the intersection of Izmit and Düzce earthquake ruptures, Uchida *et al.* (2019) observed repeating earthquakes in 2007 and 2013. Utilizing three ocean bottom seismometers deployed in the Western high, offshore Tekirdağ, similar observations were made (Yamamoto *et al.* 2019). Observations on the Main Marmara Fault are limited due to the sparseness of geodetic data and seismic activity. Yet the depth of seismogenic zone is determined to be approximately 18 km (Wollin *et al.* 2018). The last major earthquake along the Marmara section of the NAFZ including the Princes' Islands Segment south of Istanbul occurred in 1766. The absence of microseismicity (Bohnhoff *et al.* 2013) and geodetic studies there indicate a locked status (Ergintav *et al.* 2014) with the locking depth being located at  $\sim 10$  km. This segment alone is able to produce an  $M \sim 7$  earthquake (Hergert and Heidbach 2010, Bohnhoff *et al.* 2013). Recently, employing borehole strain sensors, an ultra-slow earthquake (equivalent to a  $M \sim 5.8$  earthquake) was observed offshore Yalova (Martinez-Garzon *et al.* 2019), (see also Figure 1a, red star). In INSAR (Interferometric Synthetic Aperture Radar) studies, shallow aseismic creep is observed in the eastern

of the Marmara section of the NAFZ, in the Izmit and Ismetpasa segments. Çakır *et al.* (2012) observed aseismic creep at the surface rupture between the Izmit and Akyazı fault sections based on InSAR analysis of Envisat satellite images between the years 2003-2009. This result is interpreted as post-seismic fault creep since no similar observation exists prior to the earthquake. Aslan *et al.* (2019) report that this segment still exhibits aseismic creep at a decaying rate 19 years after the earthquake. A month-long creep event is reported in December 2016 with an amplitude of approximately 10 mm, which indicates an irregular aseismic creep behavior (Aslan *et al.* 2019). The eastern part of Izmit rupture attracted less attention whilst the west (Sea of Marmara, e.g., Main Marmara Fault, Princes' Islands Segment) is sampled densely with variety of sensors. We recognized a salient behavior in one seismic sensor while searching for a correlation between the observed shallow creep and seismic activity. The seismic instrument employed in this study is located at the northeast of Lake Sapanca in Serdivan, in the close proximity of 1999 Izmit rupture. Lake is a pull-apart basin formed as a result of the dextral strike-slip character of NAF. Observed seismic activity is framing two micro earthquakes occurred to the south of lake. In this study, we investigate the reasons due to this seismic activity. One of the Event-clusters (Event-2-cluster in 2015) observed in this study coincides with one of these bursts (see Figure 13a in Aslan *et al.* 2019). However, there is no creep data available for the other Event-cluster occurred in 2018. Both activities are not correlated with any other triggering source such as environmental anomalies or nearby power plants. Our results are limited since these observations are made only in one station.

## 2. Data and Analysis

Data analyzed in this study are recorded at a single seismic instrument, SAUV, which is located at the NE of Lake Sapanca, at  $40.7401^{\circ}\text{N}$   $30.3271^{\circ}\text{E}$  (Figure 1b).

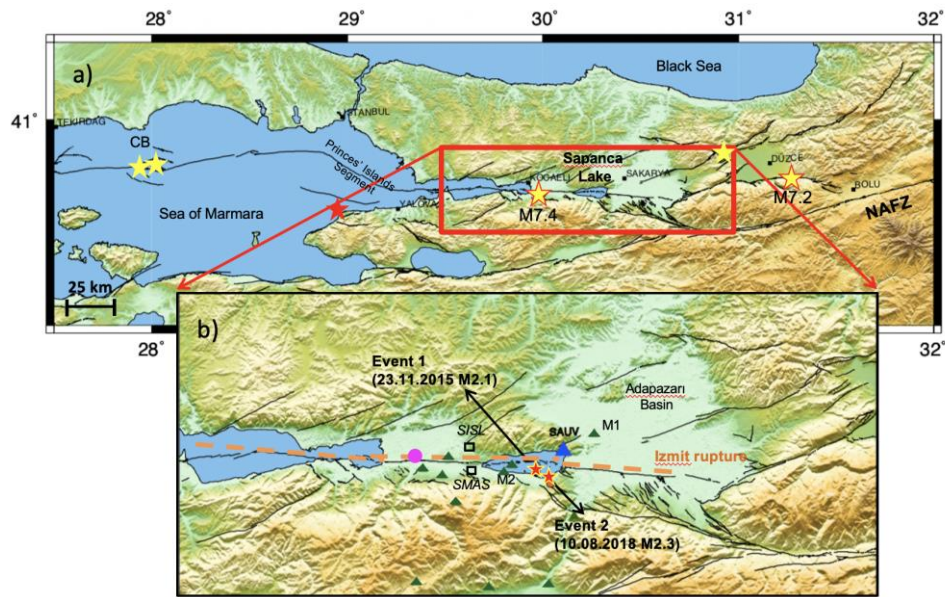


**Figure 1.** a) Hypocenters of 1999 Izmit-Gölcük and Düzce earthquakes are shown in yellow stars with red frames. Slow earthquake, magnitude M5.8, observed offshore Yalova Lake and repeating earthquakes observed in Central Basin on the Main Marmara Fault and on Düzce segment are shown in red and yellow stars, respectively. b) The blue triangle stands for the seismic sensor, SAUV, green triangles for the meteorological stations, and pink circle for the observed creep event. (NAFZ: North Anatolian Fault Zone, CB: Central Basin). As seen above, the seismic station SAUV is located on the 1999 Izmit rupture. Black squares represent the locations of GPS stations SMAS and SISL.

The seismic instrument is equipped with a Güralp CMG-6T sensor. Data are sampled at 100 Hz. Seismic activity observed in continuous waveform recordings allowed to identify two seismic sequences that occurred three years apart, but on the exact same location. The first cluster occurred on 23.11.2015 (hereafter Event 1), framing a period before and after an earthquake of M2.1 that was located at 40.7067°N/30.2685°E, according to the catalogue provided by Kandilli Observatory and Earthquake Research Institute (KOERI). The second cluster, occurred on 10.08.2018 (hereafter Event 2), again related to an earthquake at 40.62865°N 30.2995°E of M2.3, according to KOERI (Figure 1b, red stars framed in yellow). Both hypocenters are located in the south of Lake Sapanca. Raw data recorded on the vertical component can be seen in Figure 2, with respective frequency-time plots. Most of the energy is focused at frequency range 5-20 Hz. Event 2 occurred at 00:10:11 UTC on 10.08.2018, at a depth of 5.7 km. Two events were

detected preceding the main event and 15 more events occurred after.

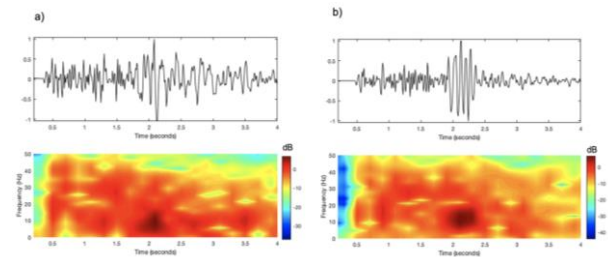


**Figure 2.** Two events observed at seismic station SAUV are shown. a) Upper panel: raw data recorded at SAUV on 23.11.2015. The waveforms are normalized. Lower panel: time-frequency plot. b) Same as a) for second event occurred on 10.08.2018.

The first event is detected two hours before the main event and the activity lasted for two hours. The Event 1 occurred at 03:47:20 UTC on 23.11.2015, at a depth of 5.7 km. The total number of events detected in the vicinity, on this day is 37 in total, 15 of them were preceding the main event. The sequence starts 20 minutes before and lasts

one hour after the occurrence of the main event. The length of the waveforms is in average 4 seconds long and S-P differential time is approximately 1.5 seconds. Figure 3 shows the waveforms exhibiting good correlation. Interestingly, the main event –Event 1- is not among these waveforms, since the waveform cross-correlation coefficient calculated with the other waveforms is small, reflecting that the waveforms are not identical. Waveforms are detected manually. Such activity is only observed if the main event occurred close to station SAUV, in and around Lake Sapanca. The observed events occurred at nighttime. Since there are several small-scale hydroelectric power plants in the near vicinity, along Sakarya River, signal to noise ratio of waveforms is comparatively low during daytime. It is an acknowledged fact that quarries are active during daytime and out of the area of observed seismic activity (Townsend 2014). To better determine the similarity of waveforms, we calculated the coherence between the 3-second-long signals framing the P- and S-wave onsets. An unfiltered waveform is divided into six segments with a 50% overlap and magnitude squared coherence is calculated,  $(coh(\omega) = |P_{xy}(\omega)|^2 / P_{xx}(\omega)P_{yy}(\omega))$ , where  $P_{xy}$  is the cross power spectral density,  $P_{xx}$  and  $P_{yy}$  are power spectral densities of two time series ( $x$  and  $y$ ) at frequency  $\omega$ . The coherence of Event 1

with the cluster on the same day and Event-2-cluster is calculated (Figure 4a, b). The coherence of Event 2 with the cluster on the same day and the Event-1-cluster is calculated (Figure 4c, d).

Within the frequency band of 2-10 Hz, the waveforms in the clusters exhibit high similarity with the corresponding main events. The two main M2.3 and M2.1 events might have triggered the same patch producing waveforms with high coherence (0.8-0.9) in the frequency band of 2-10 Hz. Another method to investigate the similarity between the waveforms is cross-correlation (Uchida and Bürgmann 2019). The correlation coefficients ( $C(\tau) = \int_1^N f_x(t)f_y(t + \tau)$ ; where  $f_x$  and  $f_y$  are two waveforms,  $N$  number of samples and  $\tau$  lag time.) are calculated between approximately 3-second-long waveform filtered between 2-10 Hz. As seen in Figure 5, the preceding events exhibit high correlation coefficients with the main event. As the occurrence time increases the correlation coefficient between the main event and the waveform decreases. In Event-1 cluster, one preceding event has a CC (cross-correlation) coefficient of 0.62 and the final 8 events have CC coefficients varying between 0.58 and 0.75. In Event-2 cluster the CC coefficients are varying between 0.7 and 0.9, only the last one is 0.56.

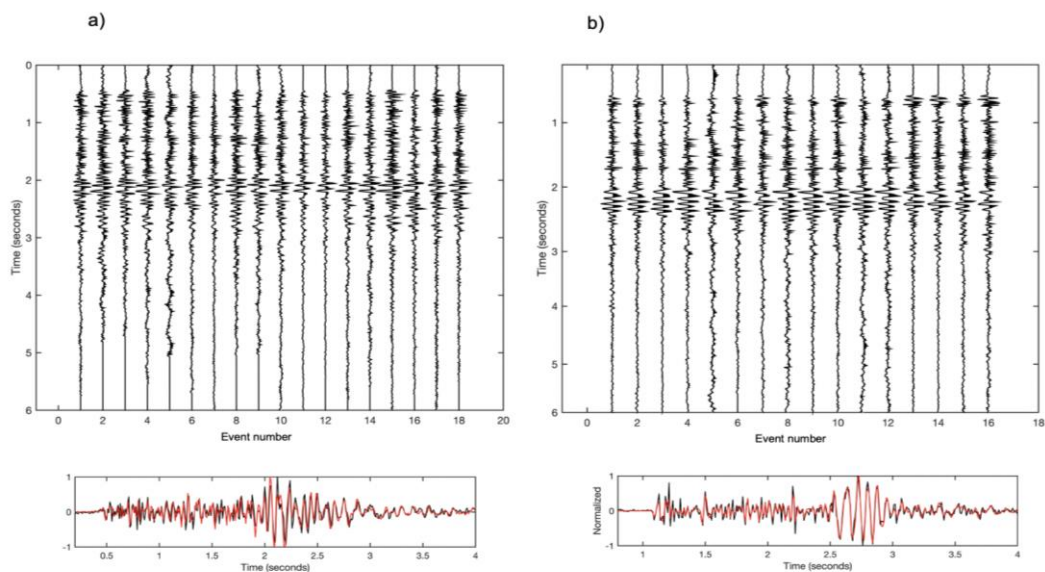


**Figure 3.** The two observed cluster of events. Data are band-pass filtered between 1-25 Hz. a) Upper panel: Event-1-cluster, Lower panel: Stack of events before the main event (in black) and after the main event (in red), b) Same as a) but for Event-2-cluster.

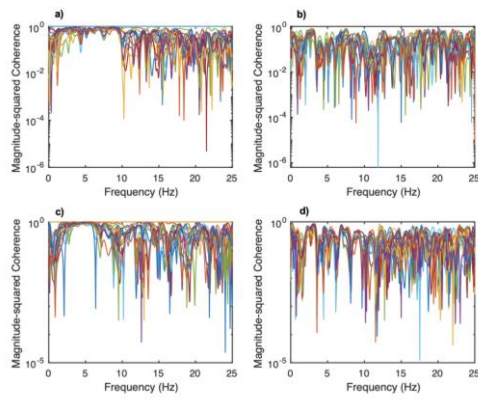


**Figure 4.** Coherency plots. Coherence between Event 1 and a) each event in Event-1-cluster and b) Event-2-cluster. Coherence between Event 2 and c) each event in Event-2-cluster and d) Event-1-cluster. Waveforms are unfiltered. Each colored solid line represents the coherence between a pair.

### 3. Correlation with environmental data

Environmental anomalies such as temperature variations, atmospheric pressure changes may produce additional unwanted transient/noise in data. It is essential to avoid temperature variations in long period seismometers using isolation techniques. Seismic instrument SAUV is equipped with a Gralp CMG-6T sensor in which thermal isolation is important, which there is no information on that. Especially, atmospheric pressure changes are difficult to avoid since they are indistinguishable (Townsend 2014). To determine whether the observed events are associated with an environmental anomaly, we investigate temperature, rainfall and pressure data during the month October in 2015 and the month August in 2018. Two close meteorological stations are considered (Figure 1b, M1 and M2). The total pressure, rainfall and temperature data per day recorded at stations M1 and M2 are shown in Figure 6. The earthquakes are indicated with a red arrow. Since the meteorological data are sampled with lower rate (hourly), it is difficult to state a correlation. Amount of rain exhibits an increase on the previous and same day with Event 2. On the day of Event 1, there is no variation in rainfall and temperature trend. On the other hand, it can be clearly seen that there is a variation in atmospheric pressure in both stations. Especially, a sharp variation in pressure data is observed in the closest station (M1) on Event 2-day. However, this information is not enough to draw a conclusion on

the correlation between atmospheric pressure and seismic observations.

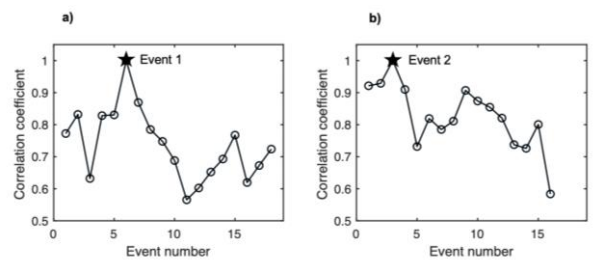


**Figure 5.** Cross-correlation coefficients calculated for each waveform a) in Event-1 cluster with Event 1 (black star) and b) in Event-2 cluster with Event-2 (black star). Events within each cluster is sorted according to their occurrence time. Waveforms are band-pass filtered between 2-10 Hz.

### 4. Epicenter estimation using single-station data

In seismology, usually seismic phase observations from several, well-distributed stations are needed to locate earthquakes. Since, our observations are limited to only one station, we perform a basic implementation of one three-component sensor to determine epicenters (the surface projection of the hypocenter which is the 'real' location at depth). P-wave particle motion is polarized in vertical plane containing the station and earthquake epicenter. The back azimuth of an event, the direction angle from epicenter to station, can be calculated using the amplitude ratio,  $atan(A_{EW}/A_{NS})$ , of E-W and N-S horizontal components (Nakamura 1988, Lockmann and Allen 2005). To get the correct back azimuth, the first motion polarity of the P wave on the vertical component is also determined since there is an ambiguity of 180°.

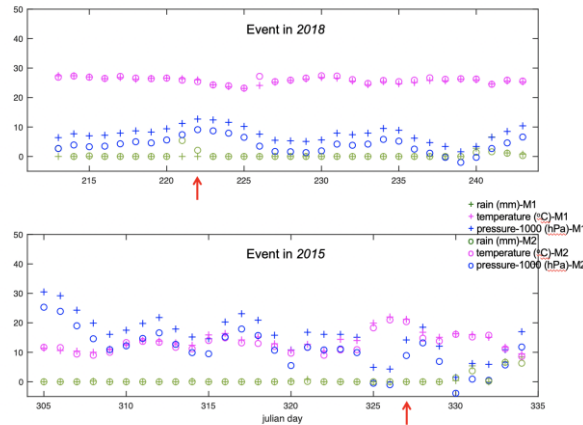


**Figure 6.** Temperature, rain and atmospheric pressure data recorded in M1 and M2 stations shown in Figure 1b. Red arrow indicates the day of the main events in 2015 and 2018.

Similarly, the apparent angle of incidence can be calculated,  $atan(A_R/A_Z)$ , where  $A_R = \sqrt{A_{EW}^2 + A_{NS}^2}$  and  $A_Z$  is the amplitude of the vertical component (Havskov and Ottemöller 2010). With the known locations of Event 2 and station SAUV, the azimuth can be calculated as  $203^\circ$ . Using this single station approach, a value of  $189^\circ$  is found.

The particle motions of the small events observed in this study are not stable since they are recorded at a station located on a tectonically complex region. Therefore, this technique is applied to a stack of clusters. For Event-2-cluster, the two small events before the main event and the ones following are stacked. The back azimuth direction estimates of  $203^\circ$  (approximately, 40.6407N 30.2717E) and  $206^\circ$  (approximately, 40.6495N 30.2688E) are found, respectively. In case of Event 1, with known locations of the event and station, the azimuth is calculated to be  $213^\circ$ . In Event-1-cluster, the sum of the events preceding the main event and the ones following are stacked and  $190^\circ$  (approximately, 40.6400N 30.3038E) is found for both (Figure 6). Moreover, taking into account the S-P times of the observed seismic events, we can estimate a region where these small events may be occurring. The velocity model in Karabulut *et al.* (2011) is taken into account (depth(km)/ $V_p$ (km/s): 0/3.27; 12/6.15; 24/6.84; 36/7.89). The estimated region for these events likely to originate from is shown as circles with a radius determined using the well-known formula  $R = t_{S-arrival} - t_{P-arrival} (V_p V_s / (V_p - V_s))$  in Figure 7.

For Event 2, the S-P times vary between 1.27 and 1.44 seconds (Figure 7, red circles). For Event 1, S-P times vary between 1.28 and 1.37 seconds (gray circles). According to the formulations of Savage (1990), the deformation at the surface produced during the earthquake cycle can be calculated considering an elastic half space model. If the locking depth (D) of the fault is approximately 17km (Schmittbuhl *et al.* 2016) in Izmit-Sapanca segment, surface deformation can be estimated as D/3. The approximate region for surface deformation along the fault is denoted by black dashed lines in Figure 7. The calculated back azimuths and hypocenter locations of stacked events suggest, that the recorded seismicity likely originates from the same area as corresponding main events and located approximately within the surface deformation zone (Figure 7). In such a setting, one can identify recurrent slip on the same seismic patch using repeating earthquakes, providing information on fault creep if sufficient data exist.

### 5. Discussion and Conclusions

In pursuit of the shallow creep observation along Izmit-Sapanca segment, we analyzed seismic waveforms in order to find a correlation with the seismic activity. The number of stations is less in this region compared to Sea of Marmara segments where a magnitude  $M > 7$  earthquake is expected.

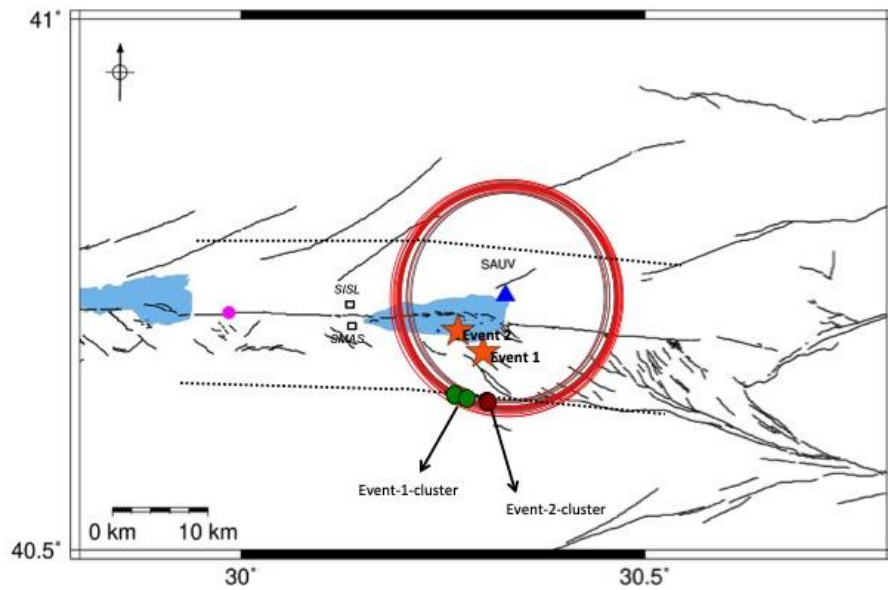


**Figure 7.** The estimated regions for the Event-1- (red circles) and Event-2-cluster (gray circles). The approximate region for surface deformation along the fault is also shown (black dashed lines). The dark green and red filled circles represent the estimated locations (back azimuths) of each event in the clusters, in Event-1 and Event-2, respectively.

With a careful and thorough analysis of recordings of a seismic sensor located at the center of 1999 Izmit earthquake rupture, two clusters of repeating events are recognized related to additional microearthquakes in the same area (Event-1 and Event-2) of magnitudes 2.1 and 2.3. Since, they are only observed in one station, possible investigations are limited. Data between the years 2013 and 2018 are scanned and only one station (SAUV) exhibits such an activity. Employing one three-component station (SAUV), we calculate the direction of angle from the epicenter to station and determine that the source of these events is located at the south of the lake within the deformation zone (Figure 7). Moreover, the correlation coefficient between the 3-second-long waveforms of the main event and events in the corresponding cluster is calculated within the frequency band 2-10 Hz. The events which occurred closer in time to the main event exhibit high CC coefficient ( $>0.7$ ) with one exception in Event-1 cluster. Within the same frequency band, the coherency values vary between 0.8 and 0.9. The timing of Event-1-cluster coincides with a

creep anomaly, reflecting that the energy release on Izmit-Sapanca segment may take place both aseismically and seismically. Repeater sources, which are not located on major plate boundaries, cause small-scale stress perturbations. These sources are tides and slow slip, linked to the presence of fluids. Another source for repeating seismicity that can cause low stresses is a weak host rock in a fractured or less consolidated part of shallow crust (Frank *et al.* 2016). The seismic station SAUV is located on the alluvial deposits near Adapazarı Basin. Using a dense array of almost 70 seismic sensors, deployed in the region between the years 2012 and 2013, Altuncu-Poyraz *et al.* (2016) observed a foreshock/aftershock activity related to a M4.1 earthquake in Serdivan. They identified an unmapped NW-SE trending secondary fault located to the north of Izmit-Sapanca segment near station SAUV. It is important to detect the full seismic cycle pre-, main and aftershocks even at the smallest magnitude in order to understand the triggering process and how seismic activity will proceed in earthquake prone regions. Therefore, to better estimate the characteristics of the fault zone

and make more reliable seismic risk assessments, this region needs to be monitored densely, as well as Sea of Marmara segments.

## 6. References

- Altuncu-Poyraz, S., Teoman M.U., Türkelli, N., Kahraman, M, Cambaz, D., Mutlu, A., Rost, S., Houseman, G.A., Thompson, D.A., Cornwell, A., Utkucu, M., Gülen, L., 2015. New constraints on micro-seismicity and stress state in the western part of the North Anatolian Fault Zone: Observations from a dense seismic array, *Tectonophysics*, **656**, 190–201. <https://doi.org/10.1016/j.tecto.2015.06.022>.
- Aslan, G., Lasserre, C., Cakir, Z., Ergintav, S., Özarpaci, S., Dogan, U., et al., 2019. Shallow creep along the 1999 Izmit earthquake rupture (Turkey) from GPS and high temporal resolution interferometric synthetic aperture radar data (2011–2017). *Journal of Geophysical Research: Solid Earth*, **124**, 2218–2236. <https://doi.org/10.1029/2018JB017022>.
- Barka, A., Akyüz, H. S., Altunel, E., Sunel, G., Çakir, Z., Dikbas, A., Yerli, B., Armijo, R., Meyer, B., de Chabaliér, J. B., Rockwell, T., Dolan, J., Hartleb, R., Dawson, T., Christofferson, S., Tucker, A., Fumal, T., Langridge, R., Stenner, R., Lettis, W., Bachhuber, J., and Page, W., 2002. The Surface Rupture and Slip Distribution of the 17 August 1999 Izmit Earthquake (M 7.4), North Anatolian Fault, *Bulletin of Seismological Society of America*, **92**, 43-60, <https://doi.org/10.1785/0120000841>.
- Bohnhoff, M., Dresen, G., Ellsworth, W.L., Ito, H., 2010. Passive seismic monitoring of natural and induced earthquakes: Case studies, future directions and socio-economic relevance, in *New Frontiers in Integrated Solid Earth Sci., Int. Yr. Planet Earth*, 261-285, eds Cloetingh, S., Negendank, J., Springer, [https://doi.org/10.1007/978-90-481-2737-5\\_7](https://doi.org/10.1007/978-90-481-2737-5_7).
- Bohnhoff, M., Bulut, F., Dresen, G., Malin, P. E., Eken, T., Aktar, M., 2013. An earthquake gap south of Istanbul. *Nature Communications*, **4**, 1999. <https://doi.org/10.1038/ncomms2999>.
- Cakir, Z., Ergintav, S., Ozener, H., Dogan, U., Akoglu, A. M., Meghraoui, M., Reilinger, R., 2012. Onset of aseismic creep on major strike-slip faults., *Geology*, **40** (12), 1115–1118. <https://doi.org/10.1130/G33522.1>.
- Ergintav, S., R. E. Reilinger, R. Çakmak, M. Floyd, Z. Cakir, U. Doğan, R. W. King, S. McClusky, and H. Özener, 2014. Istanbul’s earthquake hot spots: Geodetic constraints on strain accumulation along faults in the Marmara seismic gap, *Geophysical Research Letters*, **41**, 16, 5783–5788. <https://doi.org/10.1002/2014GL060985>.
- Frank, W.B., Shapiro, N.M., Husker, A.L., Kostoglodov, V., Campillo, M., 2016. Repeating seismicity in the shallow crust modulated by transient stress perturbations, *Geology*, **786**, 105-110. <https://doi.org/10.1016/j.tecto.2016.09.003>.
- Havskov, J. and Ottemöller, L., 2010. Location. In *Routine Data Processing in Earthquake Seismology*, 101-149. The Netherlands: Springer. ISBN: 978-90-481-8696-9. <https://doi.org/10.1007/978-90-481-8697-6>.
- Hergert, T. and Heidbach, O., 2010. Slip-rate variability and distributed deformation in the Marmara Sea fault system, *Nature Geoscience*, **3**(2), 132–135. <https://doi.org/10.1038/ngeo739>.
- Hussain, E., Wright, T.J., Walter, R.J., Bekaert, D., Hooper, A., Houseman, G.A., 2016. Geodetic observations of postseismic creep in the decade after the 1999 Izmit earthquake, Turkey: implications for a shallow slip deficit, *Journal of Geophysical Research-Solid Earth*, **121**(4), 2980-3001. <https://doi.org/10.1002/2015JB012737>.
- Karabulut, H., Schmittbuhl, J., Ozalaybey, S., Lengliné, O., Komec-Mutlu, A., Durand, V., Bouchon, M., Daniel, G., Bouin, M., 2011. Evolution of the seismicity in the eastern Marmara Sea a decade before and after the 17 August 1999 Izmit earthquake, *Tectonophysics*, **510**, 17– 27. <https://doi.org/10.1016/j.tecto.2011.07.009>.
- Lockmann A.B., Allen, R.M., 2005. Single station earthquake characterization or early warning, *Bulletin of Seismological Society of America*, **6**, 2029-2039. <https://doi.org/10.1785/0120040241>.
- Martínez-Garzón, P., Bohnhoff, M., Mencin, D., Kwiatek, G., Dresen, G., Hodgkinson, K., Nurlu, M., Kadiroglu, F.T., Kartal, R.F., 2019. Slow strain release along the eastern Marmara region offshore Istanbul in conjunction with enhanced local seismic moment release. *Earth and Planetary Science Letters*, **510**, 209- 218. <https://doi.org/10.1016/j.epsl.2019.01.001>.

- Nakamura, Y., 1988. On the Urgent Earthquake Detection and Alarm System (UrEDAS), Proc. 9th World Conference on Earthquake Engineering VII, Tokyo, Japan, 2-9 August 1988, 673-678.
- Savage, J. C., 1990. Equivalent strike-slip earthquake cycles in half-space and lithosphere-asthenosphere earth models, *Journal of Geophysical Research*, **95**, 4873-4879.  
<https://doi.org/10.1029/JB095iB04p04873>.
- Schmittbuhl, J., Karabulut, H., Lengline, O., Bouchon, M., 2016. Long- lasting seismic repeaters in the central basin of the main marmara fault, *Geophysical Research Letters*, **43** (18), 9527-9534  
<https://doi.org/10.1002/2016GL070505>.
- Townsend, B., 2014. Symmetric Triaxial Seismometers. In: Beer, M., Kougioumtzoglou, I., Patelli, E., Au, IK. (eds) *Encyclopedia of Earthquake Engineering*, 1-19. Springer, Berlin, Heidelberg.  
[https://doi.org/10.1007/978-3-642-36197-5\\_194-1](https://doi.org/10.1007/978-3-642-36197-5_194-1).
- Uchida, N and Bürgmann, R., (2019) Repeating earthquakes, *Annual Review of Earth and Planetary Sciences*, **47**(1), 305-332.  
<https://doi.org/10.1146/annurev-earth-053018-060119>.
- Uchida, N., 2019. Detection of repeating earthquakes and their application in characterizing slow fault slip, *Progress in Earth and Planetary Sciences*, **6**, 40,  
<https://doi.org/10.1186/s40645-019-0284-z>
- Wollin, C., Bohnhoff, M., Vavrycuk, V., Martínez-Garzón, P., 2018. Stress inversion of regional seismicity in the Sea of Marmara region, Turkey. *Pure and Applied Geophysics*, **176**, 1269-1291.  
<https://doi.org/10.1007/s00024-018-1971-1>.